SAND2023-04899C

Proceedings of the 20th International Symposium on the Packaging and Transportation of Radioactive Materials

11-15 June 2023, Juan-les-Pins, France

TOWARDS UNDERSTANDING STRESS CORROSION CRACKING OF AUSTENITIC STAINLESS STEELS

R. M. Katona
Sandia National Laboratories

A.W. Knight
Sandia National Laboratories

J.M. Taylor
Sandia National Laboratories

C.R. Bryan
Sandia National Laboratories

R. F. Schaller
Sandia National Laboratories

ABSTRACT

In-situ crack growth rates were determined in sea salt brines at elevated temperatures for stainless steel 304L. It was determined that magnesium chloride dominant brines had higher measured crack growth rates in comparison to sodium chloride dominant brines. Also, the addition of magnesium nitrate was shown to decrease and subsequently stop crack growth in magnesium chloride brines. Finally, the effect of temperature was explored under nitrate bearing conditions, and while crack growth rate increased with an increase in temperature, when reduced again to the initial test temperature, crack growth ceased again.

INTRODUCTION

In many environments, austenitic stainless steels have been shown to be susceptible to stress corrosion cracking (SCC). There exists a substantial amount research of performed on the SCC of austenitic stainless steels in boiling water reactor environments (with chloride in the ppm levels) as well as standardized boiling $MgCl_2$ environments (saturated chloride). However, in coastal and near-coastal environments where the deposition of sea salt is possible on the surface of the alloys, the composition, concentration, and temperature of the salt solution will vary with environmental parameters. For example, if it is assumed that ASTM seawater is representative of the salts deposited on the surface of the alloy, the composition and concentration is dependent upon the relative humidity (RH) and temperature on the surface of the alloy [1]. At high RH values, ASTM seawater is NaCl-dominant, while at low RH values (< 65 % RH), the brine would be $MgCl_2$-dominant [1]. Thus, testing in common seawater simulants, typically 0.6 M NaCl, may not necessarily be representative of the environments of interest, especially for heated, low RH, surfaces.

One scenario under which chloride-induced SCC of stainless steel 304L (SS304L) may pose a risk is the interim storage and the eventual transport of spent nuclear fuel in SS canisters in the United States. Potential SCC of these canisters has been identified as a key knowledge gap for research [2]. For canister-relevant environments, it is likely that, due to the heat from the radioactive fuel, low

RH environments will be initially present on the surface of the canisters [3, 4]. If it is assumed that sea salts are the dominant source of salt on the surface of the canisters, then concentrated $MgCl_2$ brines would be the initial deliquescent brines to form on the surface the canisters [3, 4]. Despite significant research on in-situ crack growth rate (CGR; da/dt) determination, studies related to the high fidelity, in-situ determination of CGRs in environments representative of low RH atmospheric conditions are lacking. The goal of this paper is as follows: (i) evaluate the in-situ crack growth rate response as a function of stress intensity (K) for 76 and 40 % RH sea-salt brine (that is, a brine that would be in equilibrium with air at 76 and 40% RH) at elevated temperatures, (ii) explore loading rate influences on crack growth rate determination, (iii) assess nitrate influences on crack growth rates, and (iv) evaluate the effects of temperature on CGRs under nitrate bearing conditions.

EXPERIMENTAL

A ¾″ compact tension (CT) specimens was utilized according to ASTM E1681-03[5] and ASTM E647 [6]. CGR tests were performed under K control determined by ASTM E1457 [7]. Direct current potential drop (DCPD) measurements of CGR in-situ were performed using Ni wires with a diameter of 1 mm for the current and potential drop measurements. The wires were heat shrunk in Teflon and spot welded to the sample. The spot weld locations were epoxy coated to prevent galvanic coupling. A current of 1 A was applied to the sample and was reversed every 1 s to minimize thermoelectric effects. The absolute values of the measured potentials associated with the reversing current were averaged to obtain a single data point. The calculated crack length was used to estimate the load required to maintain the desired K level. Load adjustments were made when the K deviated from the target value by more than 0.1%. The crack growth rate (da/dt) was then calculated from the DCPD-measured crack length vs. time trace using the polynomial (n = 3) method described in ASTM E647[6]. The effect of crack tip plasticity on the mechanical driving force was not considered due to small differences in equivalent plastic (K_J) and elastic stress intensities (K_e).

The specimens were fatigue pre-cracked in laboratory air prior to solution exposure using an initial frequency of 1 Hz, $K_{max} = 14\ MPa\sqrt{m}$, and R-ratio ($K_{min}/K_{max}$) of 0.1. After initiation, crack extension in air was continued at a frequency of 1 Hz, $K_{max} = 10\ MPa\sqrt{m}$, and R-ratio of 0.1. Testing of the CT specimens was performed under full immersion conditions in an acrylic cylindrical cell mounted in a load frame. The volume of the cell was roughly 3 L. The solution in the test cell was recirculated (225 mL/min) from a 3 L external reservoir. In all tests, the corrosion potential was monitored using a silver-silver chloride (Ag/AgCl) electrode as a reference electrode. The samples were loaded via clevises (manufactured from C-276) and electrically isolated using ceramic-coated pins. After being placed in the mechanical load frame, specimens were aligned with the clevises to allow for free rotation, in compliance with the K solution boundary conditions [7]. Under full immersion conditions, two test methodologies were utilized: (i) decreasing frequency at a constant K_{max} and defined R-ratio to constant K (Figure 1(a)) and (ii) monotonically increasing K to constant K (Figure 1(b)). First, decreasing frequency tests start out at a relatively high frequency (~ 0.1 Hz) and the frequency is slowly stepped down (0.01 Hz) until constant *K* is reached, as displayed in Figure 1(a). For rising K tests, a defined loading rate (dK/dt = 0.33 $MPa\sqrt{m}/hr$) was specified until the selected K_{max} was reached and the crack extension was monitored [8]. This is shown schematically in Figure 1(b). In most cases, the rising K test is performed first.

Prior to testing in solution, a different sample was utilized to measure the crack growth rate vs. applied stress intensity relationships in air at low RH (RH < 5%). Testing in air yields a nominally linear relationship between log(da/dt) and K instead of the typical rapid increase in da/dt that is characteristic of Stage I environmentally assisted cracking (EAC). This demonstrates that such

linear increases in log(da/dt) with K are not due to real crack extension. Instead, this apparent crack growth is due to strain-induced geometric contractions of the test specimen and crack tip plasticity-induced changes in material resistivity [8] that both act to increase the DCPD-measured voltage. The assumption that the observed linear log(da/dt) vs. K relationship in low RH is not indicative of real crack growth is corroborated by fractography.

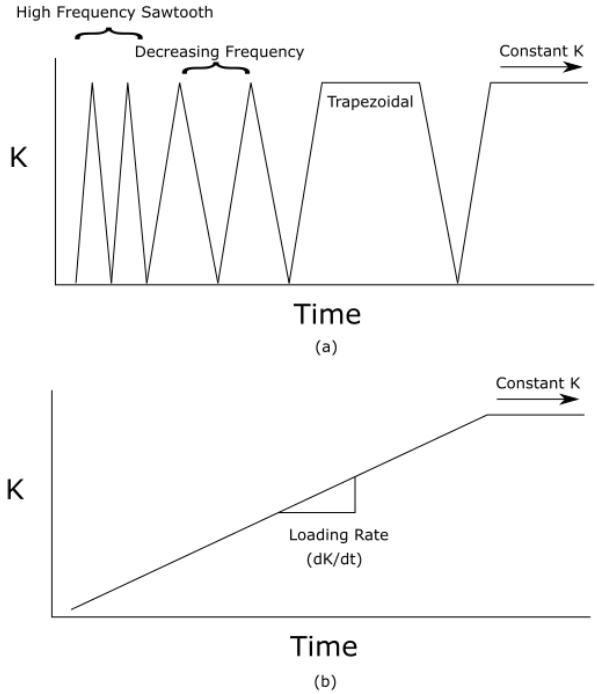

Figure 1: (a) Decreasing frequency loading protocol to constant K and (b) rising K to constant K testing methodologies.

Prior work demonstrated that the 'linear' region can be fit to an exponential equation and then subtracted from as-measured EAC growth rate to obtain the 'true' crack growth rate for a given applied stress intensity [8]. The 'linear' region from the air test was fit between 15 $MPa\sqrt{m}$ ≤ K ≤ 50 $MPa\sqrt{m}$ using least-squares regression, yielding the following relationship:

$$\frac{da}{dt} = 1.956 \cdot 10^{-8} 10^{0.0365*K} = 1.956 \cdot 10^{-8} \exp(0.0840 * K) \qquad \text{Eqn. (1)}$$

Crack growth rates for rising K tests in brine were corrected with Eqn. 1.

Following test completion, samples were sonicated in DI then methanol for 15 min. each. Next, the samples were heat tinted at a temperature of 450 °C for 1 hour and allowed to air cool. After heat tinting, the samples were reloaded into the frame in air and fatigued at the maximum exposed K (50 $MPa\sqrt{m}$), R-ratio of 0.1, and a frequency of 1 Hz for roughly 10 mm (1 cm) of crack extension. After the fatigue cycle, samples were subjected to ductile failure and torn apart for fractography analysis.

Descriptions of mechanical properties and material compositions for the sample materials are presented in Table 1 and Table 2, respectively.

Table 1: Lot information for material utilized

Lot ID	Plate #	Heat #	Form	Alloy	UTS (MPa)	YS 0.2% (MPa)	Elongation(%)	HRB
3	213104	04E28VAA	Plate	SS304L	623	292	62.9	81

Table 2: Chemical information for material utilized

Lot ID	C	Co	Cr	Cu	Mn	Mo	N	Nb	Ni	P	S	Si	Ti
3	0.017	0.234	18.1	0.412	1.782	0.414	0.08	0.014	8.03	0.037	0.001	0.236	0.002

The brine solutions utilized in this study are representative of ASTM seawater [9] at 76 % and 40 % RH [1]. The mixing formulas are presented in Table 3. For the 76 % RH brine, the sodium sulfate and boric acid were fully dissolved in the water prior to adding the other salts. All other salts besides sodium bicarbonate, including NaCl and $MgCl_2$:$6H_2O$, were added slowly while stirring. Sodium bicarbonate was added last. For the 40 % brine, the magnesium sulfate and boric acid were dissolved in water first. Second, the $MgCl_2$:$6H_2O$ was stirred in very slowly. Next, the rest of the salts were added with the magnesium carbonate added last. After the magnesium carbonate was added, the solution was stirred overnight. The solution was then gravity fed through Whatman #41 filter paper to remove any undissolved carbonate.

Table 3: Mixing formula for brines utilized

76 % RH Sea Salt		40 % RH Sea Salt	
Component	**Mass added, g**	**Component**	**Mass added, g**
NaCl	258.551	NaCl	10.423
KCl	7.001	KCl	4.619
$MgCl_2$:$6H_2O$	111.736	$MgCl_2$:$6H_2O$	1030.856
$CaCl_2$ (anhydrous)	1.306	$CaCl_2$ (anhydrous)	0.354
Na_2SO_4	29.096	$MgSO_4$	7.845
$NaHCO_3$	0.5420	$MgCO_3$	9.584
KBr	1.0177	$MgBr_2$:$6H_2O$	25.679
H_3BO_3	0.2721	H_3BO_3	5.593
H_2O	940.592	H_2O	413.583

In the test using the 40 % sea-salt brine in Table 3, once a steady CGR was achieved, $Mg(NO_3)_2$ was added in stepwise fashion, until cracking ceased.

RESULTS

A comparison of all crack growth rates vs. literature crack growth rates is presented in Figure 2. As presented, CGR values fall within literature values. Of the solutions tested, the 40 % sea salt solution has a slightly higher crack growth rate, when nitrate is not present, with respect to 76 % RH sea salt. The fastest CGR for 40 % RH sea salt was measured to be $8.87 \cdot 10^{-10}$ m/sec and was measured during rising K. The fastest CGR for 76 % RH sea salt was $1.9 \cdot 10^{-10}$ m/sec and was measured during constant K after transitioning from a rising K method.

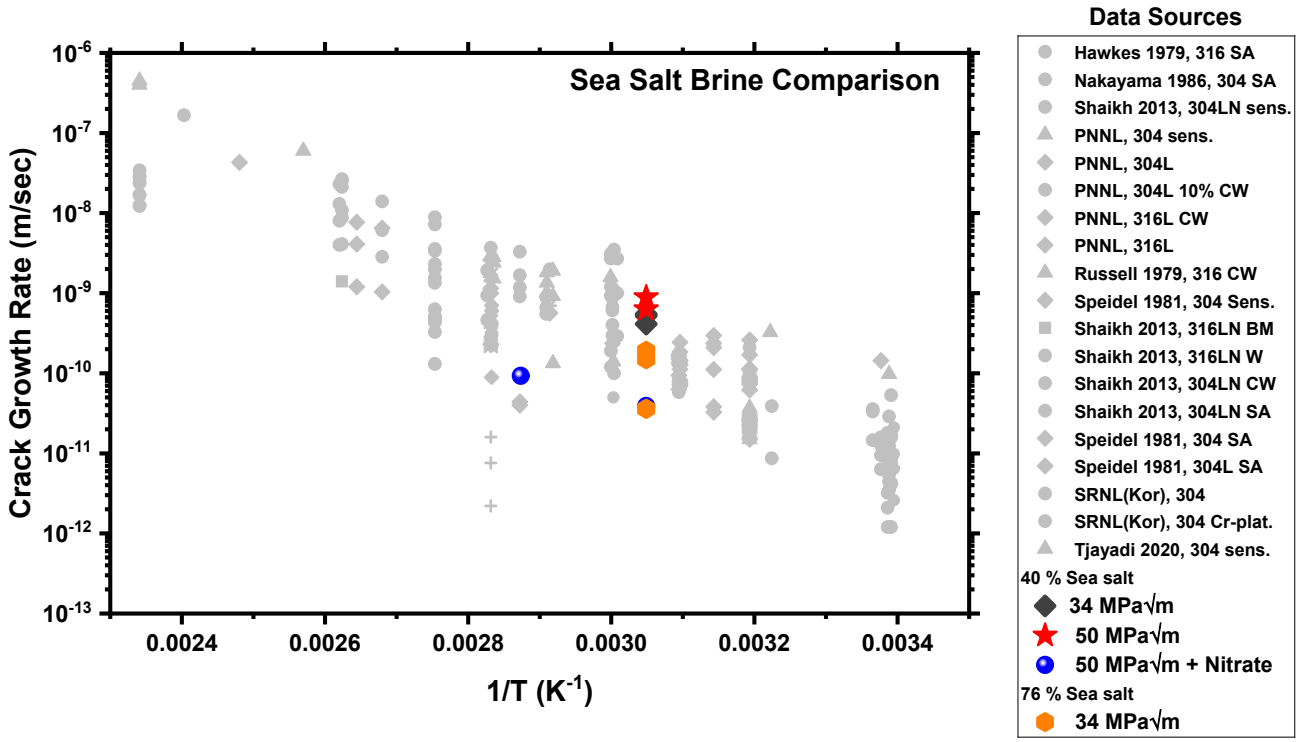

Figure 2: Comparison of measurement crack growth rates with literature values from [ref].

CGR values for 40 % sea salt showing the influence of nitrate additions and temperature increase/decrease are presented in Figure 3. As shown in Figure 3, increasing K slightly increases CGR. However, at the increased K, with the addition of nitrate to a Nitrate:chloride ratio of 1:15, the CGR decreased to roughly $3.5 \cdot 10^{-8}$ mm/sec. After the second addition of 258 g $Mg(NO_3)_2$ (for a total of 721.25 g and a nitrate to chloride ratio of 1:11), CGR ceased. During the nitrate additions, the measured OCP increased significantly from roughly -0.34 $V_{Ag/AgCl}$ to -0.26 $V_{Ag/AgCl}$ and then to -0.25 $V_{Ag/AgCl}$ during the first and second additions of nitrate respectively. After no CGR was observed with a 1:11 ratio of nitrate:chloride at 55 ˚C, the temperature was increased to 75 ˚C. After temperature stabilization, a measurable crack extension was observed and was calculated to be $2.16 \cdot 10^{-8}$ mm/sec. After exposure to 75 ˚C, the solution temperature was decreased back to 55 ˚C and there was no indicated CGR during this portion and suggests that there is no influence on CGR when decreasing temperature.

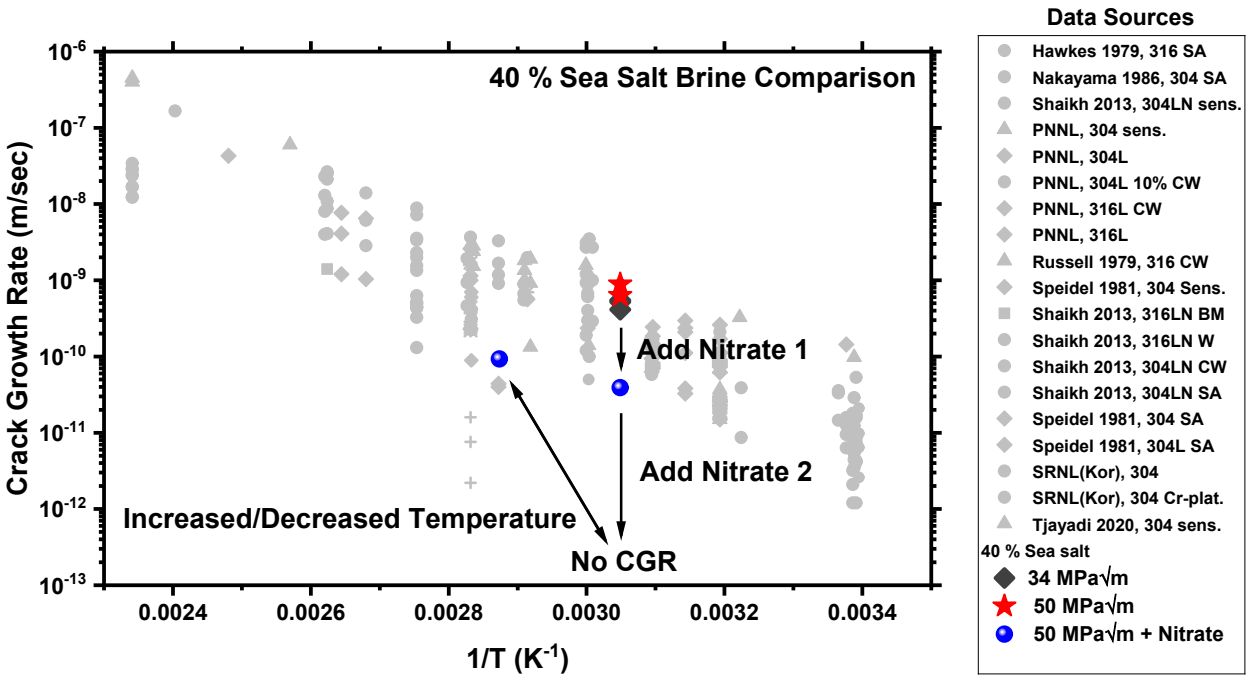

Figure 3: Comparison of measurement crack growth rates with literature values from [ref].

CONCLUSIONS

In-situ crack growth rates were evaluated on SS304L in 40 and 76 % sea salt ($MgCl_2$-dominant brine) at 55 and 75 ˚C utilizing various methods. Over various transition methods and stress intensity values, an average crack growth rate of roughly $6 \cdot 10^{-10}$ m/sec was determined for 40 % RH sea salt. This was a faster crack growth rate than 76 % RH sea salt, which had an average crack growth rate of $1.25 \cdot 10^{-10}$ m/sec. Nitrate additions at a ratio of 1:15 nitrate:chloride in 40 % RH sea salt were shown to decrease measured crack growth rate; further additions, increasing the ratio to 1:11, stopped measurable crack growth. Finally, increasing the temperature of the stopped crack to 75 ºC induced further crack growth, while returning it to the original lower temperature (55 ºC) once again caused crack growth to stop. The observations made in this paper have important testing implications for stainless steel alloys in concentrated chloride environments.

ACKNOWLEDGMENTS

Conversations with Dr. Jimmy Burns (University of Virginia), Sarah Blust (University of Virginia), Dr. Mychailo Toloczko (Pacific Northwest National Laboratories), and Brendan Nation (Sandia National Laboratories) are greatly appreciated. This article has been authored by an employee of National Technology & Engineering Solutions of Sandia, LLC under Contract No. DE-NA0003525 with the U.S. Department of Energy (DOE). The employee owns all right, title and interest in and to the article and is solely responsible for its contents. The United States Government retains and the publisher, by accepting the article for publication, acknowledges that the United States Government retains a non-exclusive, paid-up, irrevocable, world-wide license to publish or reproduce the published form of this article or allow others to do so, for United States Government purposes. The DOE will provide public access to these results of federally sponsored research in accordance with the DOE Public Access Plan https://www.energy.gov/downloads/doe-public-access-plan.

REFERENCES

1. Bryan, C.R., et al., *Physical and chemical properties of sea salt deliquescent brines as a function of temperature and relative humidity.* Science of The Total Environment, 2022. **824**(10): p. 19.
2. Teague, M., et al., *Gap Analysis to Guide DOE R&D in Supporting Extended Storage and Transportation of Spent Nuclear Fuel: An FY2019 Assessment*. 2019.
3. Bryan, C.R., et al., *FY21 Status Report: SNF Interim Storage Canister Corrosion and Surface Environment Investigations*. 2021: Albuquerque, NM, and Livermore, CA (United States). p. 199.
4. Schaller, R.F., et al., *FY2022 Status Report: SNF Interim Storage Canister Corrosion and Surface Environment Investigations* 2022, Sandia National Laboratories: Albuquerque, NM, and Livermore, CA (United States).
5. ASTM International, *E1681–03 Standard Test Method for Determining Threshold Stress Intensity Factor for Environment-Assisted Cracking of Metallic Materials*. 2008.
6. ASTM International, *E647-15 Standard Test Method for Measurement of Fatigue Crack Growth Rates*. 2015.
7. ASTM International, *ASTM E1457 Standard Test Method for Measurement of Creep Crack Growth Times in Metals*. 2020.
8. Harris, Z.D., et al., *Elucidating the loading rate dependence of hydrogen environment-assisted cracking in a Ni-Cu superalloy.* Theoretical and Applied Fracture Mechanics, 2020: p. 102846.
9. ASTM International, *D1141 Standard Practice for the Preparation of Substitute Ocean Water*, in *ASTM International*, A. International, Editor. 2013: West Conshohocken, PA. p. 1-3.